Chemistry & Biology
Article

Identification of a Small-Molecule Inhibitor of DNA Topoisomerase II by Proteomic Profiling

Makoto Kawatani,[1] Hiroshi Takayama,[1,2] Makoto Muroi,[1] Shinya Kimura,[3] Taira Maekawa,[4] and Hiroyuki Osada[1,2,*]
[1]Chemical Biology Core Facility, Chemical Biology Department, RIKEN Advanced Science Institute, Saitama 351-0198, Japan
[2]Graduate School of Science and Engineering, Saitama University, Saitama 338-8570, Japan
[3]Department of Internal Medicine, Faculty of Medicine, Saga University, Saga 849-8501, Japan
[4]Department of Transfusion Medicine and Cell Therapy, Kyoto University Hospital, Kyoto 606-8507, Japan
*Correspondence: hisyo@riken.jp
DOI 10.1016/j.chembiol.2011.03.012

SUMMARY

BNS-22, a chemically synthesized derivative of the natural plant product GUT-70, has antiproliferative activity against human cancer cells, the mechanism of which is unknown. Here, we identify a target of BNS-22 by proteomic profiling analysis, which suggests that BNS-22 belongs to the same cluster as ICRF-193, a DNA topoisomerase II (TOP2) catalytic inhibitor. BNS-22 inhibits kinetoplast DNA decatenation that is mediated by human TOP2α and TOP2β in vitro at an IC_{50} of 2.8 and 0.42 μM, respectively. BNS-22 does not affect DNA damage and antagonizes TOP2 poison-mediated DNA damage. Like ICRF-193, BNS-22 induces mitotic abnormalities, characterized by impairments in chromosome alignment and segregation, thereby causing polyploidy in HeLa cells. These results indicate that BNS-22 targets TOP2 and acts as its catalytic inhibitor.

INTRODUCTION

The promising trends of anticancer drug development programs that were initiated in the early postgenomic era have not translated into many clinical benefits. Researchers, however, have learned much about the host- and cancer-related factors that influence the prognosis of patients who are treated with drugs that have well-defined molecular mechanisms of action. To render a therapy more successful, at least one factor must be elucidated—the precise mechanism of action.

Kimura et al. (2005) reported that the natural product GUT-70, isolated from the stem bark of *Calophyllum brasiliense* in Brazil, inhibits leukemic cell growth and induces caspase-mediated apoptosis. These results prompted us to synthesize derivatives of it that have more robust biological activity; of the more than 60 derivatives of GUT-70, the compound BNS-22 fulfilled this criterion. Yet, its molecular target and mechanism of action remained unknown. A gradual and stepwise analysis of a mechanism of action typically is a long-lasting process that is accompanied by significant degree of uncertainty. Therefore, the best and, hopefully, fastest such approach is a proteomic analysis.

Affinity purification of small-molecule binding proteins using tagged probes, such as biotin conjugates and small-molecule affinity matrices, is a commonly used method (Usui et al., 2004; Teruya et al., 2005; Kawatani et al., 2008). Furthermore, various multidimensional phenotypic profiling methods have been reported to predict target proteins and mechanisms of action of bioactive small molecules, including chemosensitivity profiling of human cancer cell lines (Boyd et al., 2001; Yaguchi et al., 2006), cell morphology–based profiling (Perlman et al., 2004; Young et al., 2008), gene expression profiling (Gunther et al., 2003; Lamb et al., 2006), and chemical proteomics approaches (Bantscheff et al., 2007).

Recently, we reported a proteome-based profiling approach to predict targets of bioactive small molecules using two-dimensional fluorescence differential gel electrophoresis (2D-DIGE) (Muroi et al., 2010). This method is based on recording the comprehensive patterns of variation in proteins in HeLa cells that are treated with small molecules. Our analysis revealed that small molecules that share a molecular target, such as Hsp90 inhibitors (geldanamycin and radicicol), V-ATPase inhibitors (bafilomycin A1 and concanamycin A), and actin inhibitors (cytochalasin D and jasplakinolide), can be grouped into the same cluster. Thus, this proteomic approach is a powerful tool that can be used to classify and predict targets of bioactive small molecules.

Here, we identify a target molecule of BNS-22 by proteomic profiling: DNA topoisomerase II (TOP2). TOP2 is an essential nuclear enzyme that regulates DNA topology and many fundamental processes of DNA metabolism (Champoux, 2001; Wang, 2002; Nitiss, 2009a). TOP2 creates a transient double-strand break in one DNA molecule, through which a second dsDNA molecule is transported (Wang, 2002; Nitiss, 2009a). In mammals, there are two TOP2 isoforms, α and β, which share ~70% sequence identity and have nearly identical catalytic properties in vitro (Austin and Marsh, 1998). They have distinct patterns of expression and physiological functions in mammalian cells (Isaacs et al., 1998). TOP2α expression is cell cycle regulated, peaking in G2/M phase, and is essential for all cells. In contrast, TOP2β expression is independent of the cell cycle and occurs in proliferating and differentiated cells. TOP2β is required for proper neural development in mice (Yang et al., 2000) but is dispensable in other cell types. TOP2α has been proposed to function in growth-dependent processes, such as DNA replication and chromosomal segregation, whereas TOP2β appears to regulate transcription (Ju et al., 2006; Nitiss, 2009a).

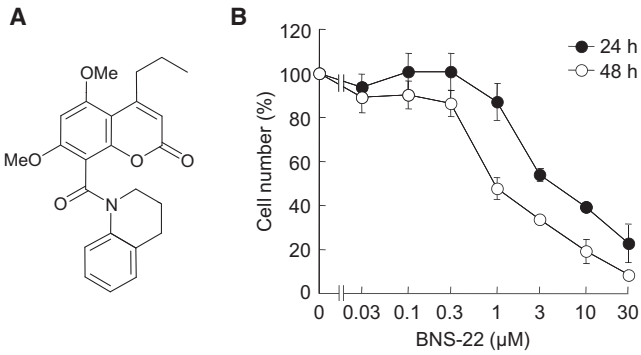

Figure 1. BNS-22 Inhibits the Growth of HeLa Cells

(A) Structure of BNS-22.

(B) Effect of BNS-22 on HeLa cell growth. HeLa cells were treated with the indicated concentrations of BNS-22 for 24 hr and 48 hr. Cell growth was analyzed by WST-8 assay. Cell number (%) indicates the percentage of control. Data are shown as the mean ± SD (n = 3).

See also Figure S1.

In addition to its critical functions, TOP2 is a clinically important target for cancer chemotherapy, and TOP2 inhibitors are vital components in many therapeutic regimens (Nitiss, 2009b; Pommier et al., 2010). TOP2-targeted inhibitors are classified into two groups according to their mechanism of action: TOP2 poisons and catalytic inhibitors. TOP2 poisons, including etoposide (VP-16), daunorubicin, mitoxantrone, and amsacrine, stabilize the reversibly covalent TOP2-DNA complex—termed the cleavable complex—that leads to DNA double-strand break formation, resulting in cancer cell death (Wilstermann and Osheroff, 2003). In contrast, TOP2 catalytic inhibitors block the catalytic center of the enzyme without any association with the formation of cleavable complexes or DNA breaks (Andoh and Ishida, 1998; Larsen et al., 2003). Such agents include ICRF-193 and the structurally related bisdioxopiperazine derivatives (Tanabe et al., 1991), aclarubicin (Jensen et al., 1990), fostriecin, merbarone, suramin, novobiocin, NSC35866 (Jensen et al., 2005), and QAP 1 (Chene et al., 2009). ICRF-193, for example, blocks the intrinsic ATPase activity of TOP2 and traps the enzyme on DNA in its closed clamp form (Roca et al., 1994).

Our data indicate that the TOP2 is the target of BNS-22, as predicted by proteomic profiling, and its mechanism of action entails the inhibition of its catalytic center.

RESULTS

Proteomic Profiling of BNS-22-Treated HeLa Cells

BNS-22 (Figure 1A) inhibited the growth of the human cervix epidermoid carcinoma cell line HeLa in a concentration-dependent manner, as evidenced by the IC_{50} values of 4.9 and 1.0 μM for the 24- and 48-hr treatments, respectively (Figure 1B; see Figure S1 available online). This result indicates that the cytotoxic effects are time dependent, which is typical for enzymatic inhibition rather than instantaneous and temporary cellular damage.

To predict the mechanism of action of BNS-22, we performed proteomic profiling of BNS-22–treated cells by 2D-DIGE. HeLa cells were treated with 10 μM BNS-22 for 18 hr, and the resulting cell lysates were subjected to 2D-DIGE (Figures S2A and S2B). The gel images were linked to our database, which contained images that were generated by 42 well-characterized small molecules. The 296 spots that matched on all gel images were quantified using the 2D-DIGE system software, as described elsewhere (Muroi et al., 2010). Then, hierarchical cluster analysis was performed, and the results were displayed in a heat map and tree diagram. As shown in Figure 2, BNS-22 was clustered with ICRF-193, a TOP2 catalytic inhibitor. In addition, our analysis distinguished between the mechanisms of action of ICRF-193 and etoposide, a TOP2 poison (Figure 2). Our data predict that BNS-22 targets TOP2 and acts as a TOP2 catalytic inhibitor, not a TOP2 poison in cells. Aclarubicin, a known DNA-intercalating agent that prevents the binding of TOP2 to DNA rather than inhibiting its activity, was not clustered with ICRF-193 (Figure 2). This is probably because of the nonspecific effect of aclarubicin, which is known to inhibit other proteins as well, such as TOP1 and the 20S proteasome (Figueiredo-Pereira et al., 1996; Larsen et al., 2003).

BNS-22 Perturbs Mitotic Spindle Formation and Induces Polyploidy

Additional experiments were performed to determine the biological effect of BNS-22 on cell cycle in HeLa cells. By flow cytometry, 24-hr treatment with BNS-22 increased the HeLa cell population in G2/M phase in a concentration-dependent manner (Figure 3A). However, exposure to 3 μM BNS-22 beyond 24 hr was accompanied by the presence of an 8C peak (Figure 3B), characteristic of polyploidal cells. Similar effects were observed in the human promyelocytic leukemia cell line HL-60 (Figure S3).

Thus, we concluded that BNS-22 affects M phase events and disturbs mitotic spindle formation. Moreover, by proteomic profiling, BNS-22 was clustered near typical antimitotic agents, such as vinblastine and nocodazole (Figure 2). To discriminate the effects of these compounds, HeLa cells were exposed to 3 and 10 μM BNS-22, 10 μM ICRF-193, or 300 nM vinblastine for 12 hr and were stained with anti-β-tubulin, anti-γ-tubulin, and DAPI to visualize spindle and chromosomal morphology. ICRF-193 and vinblastine were used as references to differentiate the mechanisms of action. Vehicle-treated control cells and BNS-22-treated cells did not differ morphologically during interphase (Figure 3C), but during mitosis, the control cells harbored a typical bipolar mitotic spindle, whereas BNS-22–treated cells developed abnormal mitotic figures, characterized by unusually distorted spindles and a failure of chromosomal alignment and segregation (Figure 3C). Similar morphological changes were induced by ICRF-193 (Figure S4A), a TOP2 reference compound that was clustered with BNS-22 by proteomic profiling; vinblastine, an antimicrotubular agent, effected dissimilar changes (Figure S4B).

BNS-22 Inhibits TOP2 Activity

To confirm whether BNS-22 inhibits TOP2 enzymatic activity, we measured the effect of BNS-22 on TOP2-mediated kinetoplast DNA decatenation. Kinetoplast DNA is a massive network that consists of thousands of interlocked circular DNA molecules. Because a transient double-strand break is necessary to release circular DNA from the network, the decatenation of kinetoplast

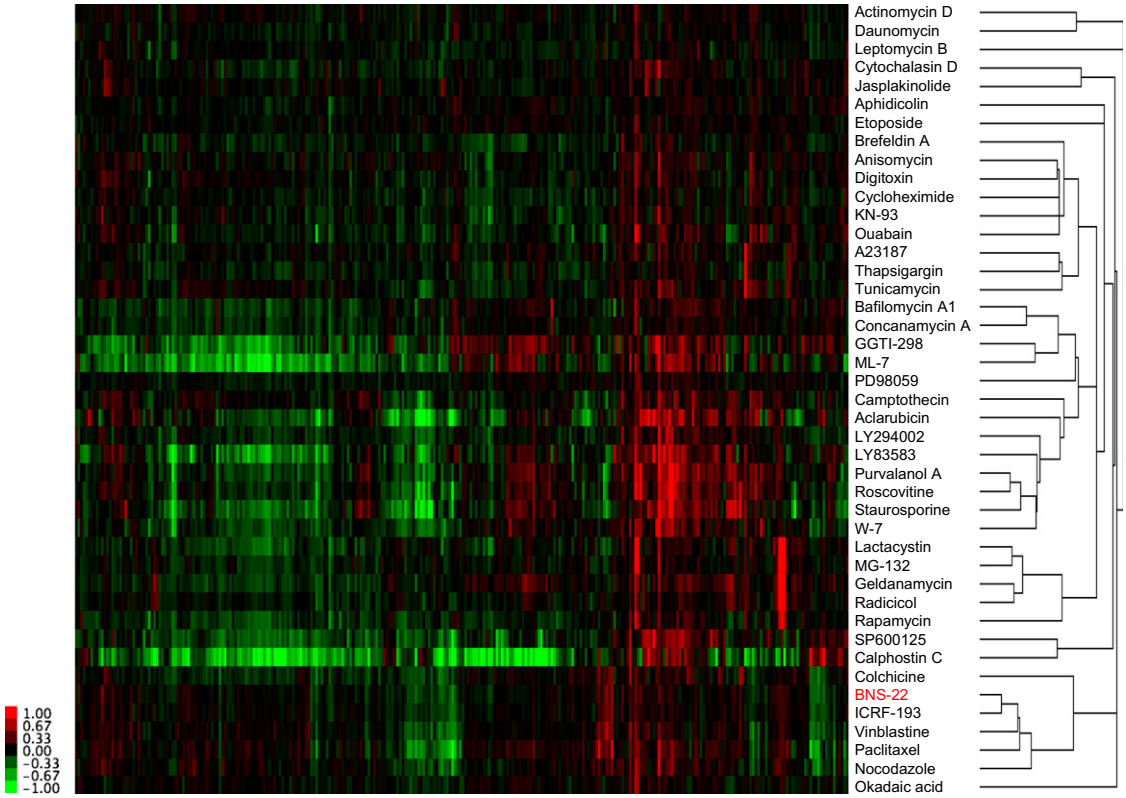

Figure 2. Clustering of BNS-22 and 42 Well-Characterized Compounds by Proteomic Analysis of HeLa Cells

HeLa cells were treated with 10 μM BNS-22 for 18 hr. Proteome analysis was performed using 2D-DIGE. Quantitative data of the 296 spots were combined with data on the 42 well-characterized compounds, and hierarchical clustering was performed. In the heat map, log-fold (natural base) of the normalized volume is shown on the colored scale.

See also Figure S2 and Table S1.

DNA is believed to be a highly specific assay for TOP2 that catalyzes double-strand passing. BNS-22, like ICRF-193, inhibited kinetoplast DNA decatenation by human TOP2α and TOP2β (Figures 4A and 4B). The mean IC_{50} value of BNS-22 for TOP2α and TOP2β, obtained from three independent experiments, was 2.8 ± 1.3 and 0.42 ± 0.09 μM, respectively, as determined by densitometric analysis.

We also observed the effect of BNS-22 on human DNA topoisomerase I (TOP1), which catalyzes topological changes in DNA by transiently introducing single-strand breaks, to determine the selectivity of BNS-22. A TOP1 inhibitor, camptothecin (100 μM), which was used as a positive control, significantly inhibited TOP1 activity, as measured by enzyme-mediated supercoiled DNA relaxation, whereas BNS-22 had no effect at concentrations up to 100 μM (Figure 4C).

BNS-22 Does Not Induce DNA Damage Associated with DNA Double-Strand Breaks

TOP2 inhibitors are classified according to their ability to induce DNA double-strand breaks due to the formation of cleavable complexes (TOP2 poisons) or not (TOP2 catalytic inhibitors), reflecting distinct mechanisms of inhibition. Moreover, TOP2 catalytic inhibitors antagonize TOP2 poison-mediated DNA damage (Ishida et al., 1991; Tanabe et al., 1991). Our proteomic profiling analysis suggested that BNS-22 acts as a TOP2 catalytic inhibitor but not as a TOP2 poison (Figure 2). To confirm this mode of inhibition, we examined the ability of BNS-22 to induce DNA damage, as measured by histone H2AX phosphorylation on serine 139, termed γ-H2AX, a hallmark of DNA double-strand breaks in cells (Rogakou et al., 1998). HeLa cells were treated with 10 μM BNS-22, ICRF-193, or etoposide for 1 hr and were stained with anti-γ-H2AX. Etoposide induced the robust formation of γ-H2AX foci, in contrast to BNS-22 and ICRF-193 (Figure 5A). To determine the antagonistic effects of BNS-22 on etoposide-mediated DNA damage, HeLa cells were pretreated with 10 μM BNS-22 or ICRF-193 for 30 min and were treated with 10 or 30 μM etoposide for 1 hr. By western blot, pretreatment with BNS-22 or ICRF-193 blocked etoposide-induced γ-H2AX accumulation (Figure 5B), suggesting that BNS-22 antagonizes TOP2 poison-mediated DNA damage.

TOP2β is preferentially degraded by the proteasome pathway after cells are exposed to TOP2 poisons or catalytic inhibitors (Mao et al., 2001; Xiao et al., 2003). We recapitulated these effects in HeLa cells that were treated with BNS-22 or ICRF-193; total cellular TOP2β levels declined markedly in a time- and concentration-dependent manner, but TOP2α levels were not significantly affected (Figures 5C and 5D). Considering the predicted mode of action by proteomic profiling and these results, we conclude that BNS-22 functions as a TOP2 catalytic inhibitor.

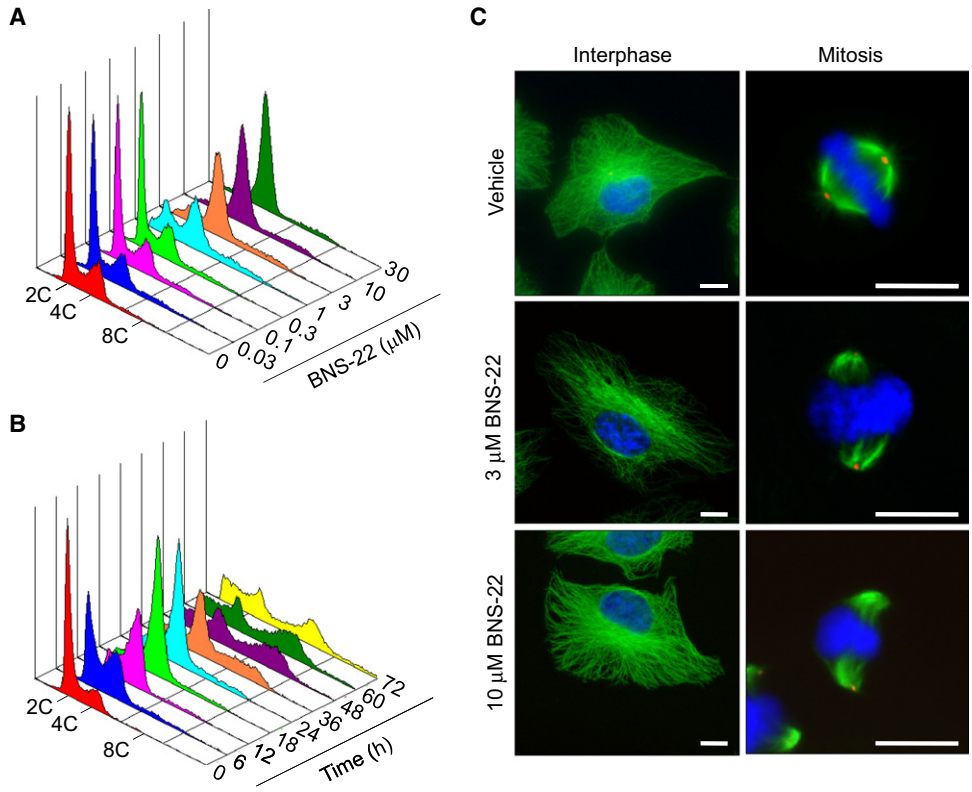

Figure 3. BNS-22 Leads to Mitotic Perturbations

(A and B) Effect of BNS-22 on cell cycle. HeLa cells were treated with the indicated concentrations of BNS-22 for 24 hr (A) or with 3 μM BNS-22 for the indicated times (B). Cells were fixed and analyzed by flow cytometry after propidium iodide staining.

(C) Effect of BNS-22 on mitotic spindle formation. HeLa cells were treated with 3 or 10 μM BNS-22 for 12 hr, fixed, and stained with anti-β-tubulin (green), anti-γ-tubulin (red), and DAPI (blue). Scale bar, 10 μm.

See also Figures S3 and S4.

To examine whether BNS-22 could bind directly to TOP2, we performed affinity precipitation assay using BNS-22–immobilized beads. Purified human TOP2α coprecipitated with BNS-22 beads, and competition was clearly observed in the presence of BNS-22 but was absent with the addition of ICRF-193 (Figure 5E). This result suggests that BNS-22 binds directly to TOP2α in a different mode from ICRF-193.

Structure-Activity Relationship of BNS-22

Structural analogs of BNS-22 were synthesized and tested for their ability to inhibit TOP2 activity (Table 1 and Figure S5). All amides of the N-heterocyclic compound—BNS-51, BNS-52, BNS-53, and BNS-54—failed to inhibit kinetoplast DNA decatenation by human TOP2α at concentrations up to 100 μM. The inhibitory activity BNS-65, an ester of BNS-22, was 3-fold lower than that of BNS-22. These results suggest that the 1,2,3,4-tetrahydroquinoline structure of BNS-22 is essential for the inhibition of TOP2 catalytic activity.

DISCUSSION

A new compound, BNS-22, was determined to possess significant antiproliferative activity against several human cancer cell lines, but its mode of action was unknown. To this end, by proteomic profiling, we found that BNS-22 targets TOP2; in contrast, its mother compound, GUT-70, a natural plant product that has antileukemic activity (Kimura et al., 2005), does not inhibit the DNA decatenation that is mediated by human TOP2α up to 100 μM (Figure S5), indicating that GUT-70 and BNS-22, despite having similar structures, have disparate molecular targets.

Agents that target TOP2 are divided into two classes: TOP2 poisons, which stabilize DNA cleavable complexes and induce DNA damage, and catalytic inhibitors, which interfere with various steps in the catalytic cycle and inhibit growth by abolishing the essential enzymatic activity of TOP2 (Larsen et al., 2003; Wilstermann and Osheroff, 2003). Bisdioxopiperazines, including ICRF-193, are believed to be specific TOP2 catalytic inhibitors, in contrast to most other compounds that are claimed to be catalytic inhibitors of TOP2. BNS-22 induces several cellular phenotypes that are characteristic of bisdioxopiperazines in cells: First, BNS-22 does not induce DNA damage, as evidenced by the lack of γ-H2AX accumulation (Figure 5A), and abrogates TOP2 poison-induced DNA damage (Figure 5B). Second, BNS-22 preferentially degrades TOP2β; TOP2α is unaffected (Figures 5C and 5D). Third, BNS-22 induces mitotic abnormalities that are characterized by the inability of chromosomes to condense and segregate (Figure 3C; Figure S4A),

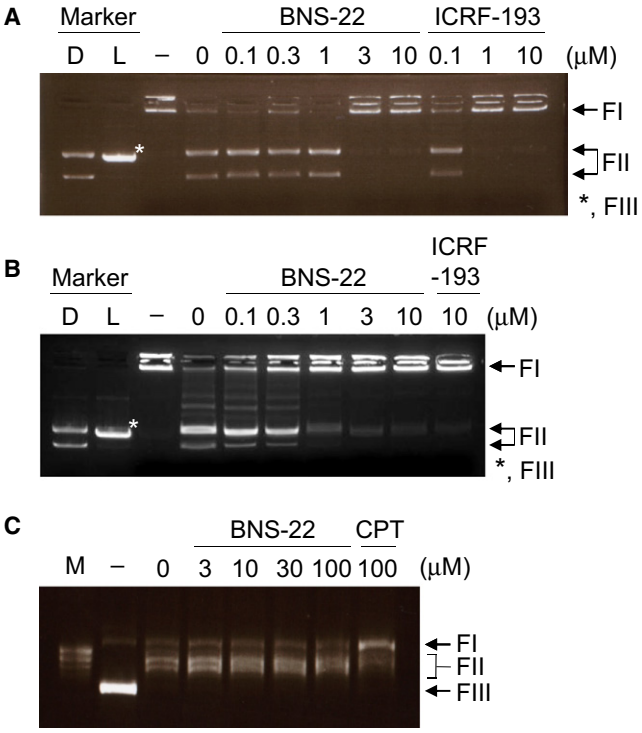

Figure 4. BNS-22 Inhibits TOP2 Activity

(A and B) BNS-22 inhibits human TOP2-mediated kinetoplast DNA decatenation. Catenated kinetoplast DNA was incubated with human TOP2α (A) or TOP2β (B) in the presence of the indicated compounds at 37°C for 30 min. DNA samples were separated by electrophoresis on a 1% agarose gel. The positions of the catenated DNA (FI), decatenated products (FII), and linear DNA (FIII) are indicated. Marker D, decatenated kinetoplast DNA; marker L, linearized kinetoplast DNA; –, no human TOP2α (A) or TOP2β (B).

(C) BNS-22 does not inhibit human TOP1-mediated supercoiled DNA relaxation. Supercoiled plasmid DNA was incubated with human TOP1 in the presence of the indicated compounds at 37°C for 30 min. DNA samples were separated by electrophoresis on a 1% agarose gel. The positions of nicked open circular DNA (FI), relaxed DNA (FII), and supercoiled DNA (FIII) are indicated. M, relaxed plasmid DNA marker; –, no human TOP1; CPT, camptothecin.

resulting in polyploidy (Figure 3B) (Muroi et al., 2010). Thus, these findings strongly suggest that BNS-22 acts as a TOP2 catalytic inhibitor in cells. Several reports suggest that bisdioxopiperazines can induce DNA damage in vitro, both in cell-free and in intact cells, although this remains controversial (Huang et al., 2001; Hajji et al., 2003; Jensen et al., 2004). The results of our study clearly show that ICRF-193 and BNS-22 do not induce DNA damage, thus contrasting the effects of the classical TOP2 poison etoposide on cells (Figures 5A and 5B); therefore, further studies are needed to evaluate the DNA-damaging activity of BNS-22 and ICRF-193 under various experimental conditions.

The inhibitory effects of BNS-22 against TOP2 are well documented, but several compounds possess dual modes of action that allow them to inhibit both TOP1 and TOP2, such as the acridine DACA, the benzopyridoindole intoplicine, the indenoquinolinone TAS-103, the camptothecin analog BN 80927, and the polysaccharide GA3P (Denny and Baguley, 2003; Umemura et al., 2003). TOP1-mediated supercoiled DNA relaxation was not inhibited by BNS-22 at concentrations up to 100 μM (Figure 4C); thus, this new compound must be classified as a specific TOP2 inhibitor, acting by blocking catalytic activity.

The catalytic cycle of TOP2 can be parsed into six discrete steps (Berger et al., 1996; Bates and Maxwell, 2007): (1) binding of TOP2 to DNA, (2) double-stranded cleavage of the DNA, (3) ATP-dependent DNA strand passage, (4) religation of the cleaved DNA, (5) ATP hydrolysis, and (6) enzyme recycling. Agents that inhibit TOP2 act through several mechanisms. For example, aclarubicin blocks enzyme-DNA binding, the initial step of the cycle (Sorensen et al., 1992), and merbarone blocks DNA cleavage (Fortune and Osheroff, 1998). Bisdioxopiperazines inhibit the catalytic cycle of TOP2 by binding near the ATP binding site and trapping the enzyme as a closed clamp on DNA (Classen et al., 2003). Because the interaction between TOP2α and BNS-22 was not inhibited by ICRF-193 (Figure 5E), BNS-22 may bind directly to TOP2 and inhibit its catalytic activity differently from bisdioxopiperazines and, as a consequence, may prevent TOP2 poison-induced DNA damage by stabilizing TOP2-DNA complexes (Figure 5B). However, further investigation is needed to determine the precise mechanism by which BNS-22 inhibits the catalytic activity of TOP2.

The identification of a mode of action is a crucial step during drug development and is important in early preclinical studies, when a substance is transferred from the in vitro to in vivo evaluation stage. The lack of such knowledge can generate disappointing results if a selected cancer does not express a molecular target for an otherwise active compound. Under such circumstances, a compound is judged to be inactive, and in general, further evaluation is halted. Mindful of the possibility for misjudgment, we developed a global system of classifying chemical entities according to their presumably chief mechanism of action, allowing us to make an informed selection of the proper object of evaluation—a tumor. This system allowed us to identify the probable mechanism of action of BNS-22 rapidly, which was confirmed in several steps. Our analysis revealed that small molecules that share a target can be classified by proteomics-based profiling (Muroi et al., 2010). With regard to BNS-22, our cluster analysis distinguished between the mode of action of ICRF-193 and etoposide, although they target the same molecule, TOP2. Our data on BNS-22 demonstrate the effectiveness of target prediction of small molecules by proteomics-based profiling. At this stage, our tool does not need to identify each spot, a generally time-consuming process in proteomic analysis. Nevertheless, characterization of the spots that are altered by treatment with small molecules might increase our understanding of biological pathways and their responses to small molecules. Expansion of the system, by increasing the number of small molecules in the database and identifying spots, will transform it into a more powerful and universal platform, not only to identify mechanisms but also to demonstrate the proof of concept of drugs that enter the clinical phase of evaluation.

TOP2 is an effective target against a wide range of malignancies, and TOP2 poisons, such as etoposide, doxorubicin, and mitoxantrone, have substantial clinical activity. Toxic side effects, however, including drug-induced secondary malignancies, have become a concern in TOP2 poison-based chemotherapy. TOP2 catalytic inhibitors have not been explored extensively

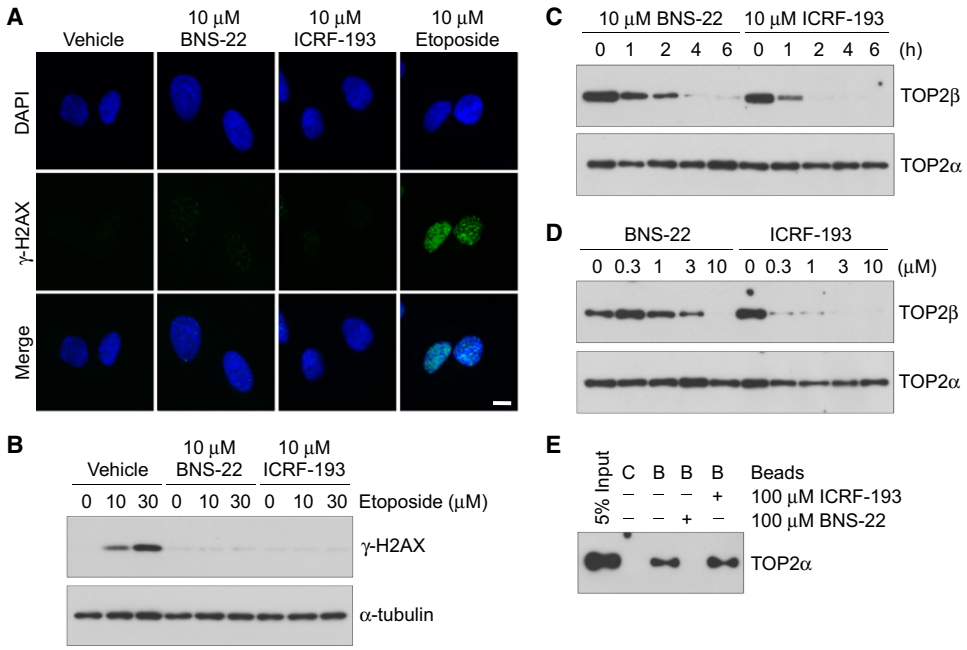

Figure 5. Assessment of Relative Potency of TOP2 Catalytic Inhibitor

(A) BNS-22 does not induce DNA damage. HeLa cells were treated with 10 μM BNS-22, ICRF-193, or etoposide for 1 hr, fixed, and stained with anti-γ-H2AX (green) and DAPI (blue). Scale bar, 10 μm.

(B) BNS-22 antagonizes etoposide-induced DNA damage. HeLa cells were pretreated with 10 μM BNS-22 or ICRF-193 for 30 min and were treated with the indicated concentrations of etoposide for 1 hr. Cell lysates were immunoblotted with anti-γ-H2AX (*top*) and anti-α-tubulin (*bottom*).

(C and D) BNS-22 decreases TOP2β levels. HeLa cells were treated with 10 μM BNS-22 or ICRF-193 for the indicated times (C) or with the indicated concentrations of BNS-22 or ICRF-193 for 6 hr (D). Cell lysates were immunoblotted with anti-TOP2β (*top*) and anti-TOP2α (*bottom*).

(E) BNS-22 binds directly to TOP2α in a different mode than ICRF-193. Purified human TOP2α was incubated with control or BNS-22 beads in the presence or absence of 100 μM BNS-22 or ICRF-193. The reactant beads were washed, and the eluted protein was immunoblotted with anti-TOP2α. C, control beads; B, BNS-22 beads.

in the clinical setting. For instance, bisdioxopiperazines were developed originally as anticancer agents but have been used principally as cardioprotecting agents in the clinic (Larsen et al., 2003). ICRF-187 has clearly been shown to prevent cardiotoxicity that is induced by doxorubicin and other anthracyclines; its ring-opened hydrolysis product is claimed to act as a strong iron chelator, diminishing the harmful effects of reactive oxygen species on heart tissue. The clinical use as anticancer agents is limited to MST-16 (Sobuzoxane), which is a prodrug of ICRF-154. It is active against hematological malignancies but has limited activity toward solid tumors (Larsen et al., 2003).

By definition, TOP2 poison-induced DNA damage can trigger many DNA repair mechanisms; cells that initiate high levels of such activity will resist these cytotoxic effects. Therefore, cancers that lack this capacity are good targets for this treatment. Conversely, TOP2 catalytic inhibitors that do not cause DNA damage should be appropriate candidates for treating cancers with fully active DNA repair systems, which mediate clinical resistance to many anticancer agents. In addition, it is unclear whether resistance to TOP2 poisons is associated with the action of TOP2 catalytic inhibitors (Larsen and Skladanowski, 1998; Larsen et al., 2003). The clinical application of TOP2 catalytic inhibitors has expanded dramatically, according to reports of the involvement of cancer-protective mechanisms in instances of clinical failure. Thus, TOP2 catalytic inhibitors might constitute a second-line treatment in patients who no longer respond to TOP2 poisons, cisplatin, and other agents.

In conclusion, we have demonstrated that BNS-22 targets TOP2 and acts as its catalytic inhibitor in cells. Furthermore, our study shows that proteomics-based profiling will aid in the identification of mechanisms of action of bioactive small molecules in future drug development and chemical genetic studies. Although additional studies are needed, particularly with regard to the molecular mechanism of inhibition by BNS-22 in the catalytic cycle of TOP2 and its in vivo antitumor efficacy, BNS-22 can be used to understand the biochemical and biological functions of TOP2 and administered as an anticancer drug in chemotherapy.

SIGNIFICANCE

Identifying the molecular target of uncharacterized bioactive small molecules is a crucial step in drug development and chemical genetic studies. Recent advances in omics studies and multidimensional analyses have allowed us to profile the effects of drugs by transcript analysis, proteomics, cell phenotype assays, and chemosensitivity. In this study, we identified the target of a small molecule, BNS-22, which has antiproliferative activity against human cancer cells, using our recently developed proteomic profiling

Table 1. In vitro inhibition of TOP2 activity by BNS-22 derivatives

Compound	BNS-22	BNS-51	BNS-52	BNS-53	BNS-54	BNS-65
Structure	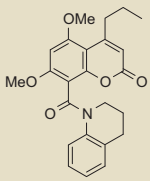	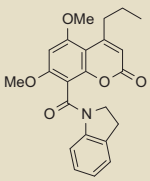	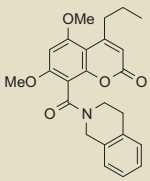	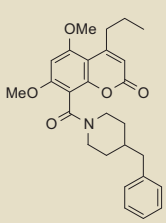	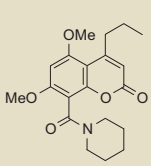	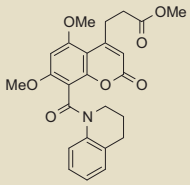
IC_{50} (μM)	2.8	>100	>100	>100	>100	8.2

Catenated kinetoplast DNA was incubated with human TOP2α in the presence of the indicated compounds at 37°C for 30 min. DNA samples were separated by electrophoresis on a 1% agarose gel. The IC_{50} value was determined by densitometric analysis. See also Figures S1 and S5.

approach. We show that BNS-22 targets TOP2 and acts as a catalytic inhibitor in a cell system. TOP2, an essential enzyme that regulates DNA topology, is a clinically important target for cancer chemotherapy. Although various TOP2 poisons, such as etoposide, have been used clinically, the catalytic inhibition of TOP2 has not been explored extensively in cancer treatment. Our study designates a structural class of TOP2 inhibitors that can be used to treat cancers that undergo high levels of DNA repair, compromising the therapeutic effects of DNA-damaging agents.

EXPERIMENTAL PROCEDURES

Materials

The following materials were used: ICRF-193 (Funakoshi); camptothecin (Calbiochem); etoposide, DAPI, anti-α-tubulin, anti-β-tubulin, and anti-γ-tubulin (Sigma-Aldrich); Alexa 488 donkey anti-mouse IgG and Alexa 568 goat anti-rabbit IgG (Molecular Probes); anti-TOP2α (MBL); anti-TOP2β (Santa Cruz Biotechnology); anti-phospho histone H2AX (Ser139) (Upstate); purified human TOP1 (Topogen), purified human TOP2α (Topogen or LAE Biotech International); and purified human TOP2β (LAE Biotech International). The synthesis of BNS-22 and its derivatives is described in Supplemental Experimental Procedures and Figure S1. All compounds were dissolved in dimethylsulfoxide (DMSO) as stock solutions, which were stored at −20°C.

Cell Culture and Cell Growth Assay

The human cervix epidermoid carcinoma cell line HeLa (RIKEN Cell Bank) was cultured in D-MEM (Invitrogen), supplemented with 10% fetal calf serum (Invitrogen), 50 unit/ml penicillin (Invitrogen), and 50 μg/ml streptomycin (Invitrogen), at 37°C in a humidified atmosphere containing 5% CO_2. HeLa cells were seeded in a 96-well culture plate, cultured overnight, and exposed to BNS-22 for the indicated times. After treatment, cell growth was measured using Cell Count Reagent SF (Nacalai Tesque) according to the manufacturer's instruction. Briefly, 1/100 volume of the WST-8 solution was added to each well, and the plates were incubated at 37°C for 1 hr. Then, cell growth was measured as the absorbance at 450 nm on a microplate reader (Perkin Elmer).

Proteome Analysis by 2D-DIGE

Proteome analysis by 2D-DIGE was performed as described elsewhere (Muroi et al., 2010). Briefly, HeLa cells were treated with the designated concentrations of BNS-22 or other inhibitors (Table S1) for 18 hr. Proteome analysis of cell lysates was performed using a 2D-DIGE system (GE Healthcare), and images of the gels were analyzed using Progenesis SameSpots (Nonlinear Dynamics). Of the 298 spots that were described in a previous report, 296 spots were detectable in all gels (Muroi et al., 2010). The volume of each spot was normalized using the average of the corresponding control values from DMSO-treated HeLa cells, and hierarchical clustering analysis was performed.

Flow Cytometric Analysis

HeLa cells were seeded in a 6-well plate and exposed to BNS-22 for the indicated times and concentrations. Cells were harvested, washed with PBS, and fixed in 70% ethanol. Cells were washed twice with PBS again and incubated with 50 μg/ml propidium iodide (Sigma-Aldrich) in PBS containing 2 μg/ml RNase A (Nacalai Tesque) in the dark for 30 min. The DNA content of the cells was analyzed on a Cytomics FC500 (Beckman Coulter).

Immunofluorescence Cell Staining

For β-tubulin and γ-tubulin costaining, cells were cultured on glass coverslips, fixed in methanol for 5 min, and washed with PBS. After blocking with 0.5% BSA in PBS for 5 min at room temperature, the slides were incubated sequentially with primary antibodies, each diluted 1:200 in PBS with 0.5% BSA, for 1 hr at 37°C and with Alexa-conjugated secondary antibodies, each diluted 1:500 in PBS with 0.5% BSA, for 45 min at 37°C.

For phospho-histone H2AX (Ser139) staining, cells that were cultured on glass coverslips were fixed in 3.7% formaldehyde for 20 min, washed with PBS, and permeabilized in 0.2% Triton X-100 in PBS for 5 min at room temperature. After blocking with 0.5% BSA in PBS for 5 min at room temperature, the slides were incubated sequentially with the primary antibody, diluted 1:200 in PBS with 0.5% BSA, for 1 hr at 37°C and with Alexa-conjugated secondary antibody, diluted 1:500 in PBS with 0.5% BSA, for 45 min at 37°C. DNA was stained with 0.1 μg/ml DAPI in PBS. Images were analyzed on a fluorescence microscope (PROVIS AX70, Olympus).

Kinetoplast DNA Decatenation Assay

TOP2 catalytic activity was measured, on the basis of ATP-dependent decatenation of kinetoplast DNA, using the TOP2 assay kit (Topogen). The reaction buffer, containing 50 mM Tris-HCl (pH 8.0), 150 mM NaCl, 10 mM $MgCl_2$, 2 mM ATP, 0.5 mM DTT, and 30 μg/ml BSA for TOP2α, or 40 mM Tris-HCl (pH 7.5), 100 mM KCl, 10 mM $MgCl_2$, 2 mM ATP, 10 mM DTT, 0.5 mM EDTA, and 30 μg/ml BSA for TOP2β, was mixed with 0.2 μg kinetoplast DNA, 1 unit of human TOP2α or TOP2β, and the indicated concentrations of the compounds in a total volume of 20 μl. After incubation at 37°C for 30 min, the reaction was terminated with the addition of 4 μl stop solution. The reaction mixtures were treated with 50 μg/ml proteinase K (Nacalai Tesque) for 30 min at 37°C to digest the protein. Samples were resolved by electrophoresis on a 1% agarose gel containing 0.5 μg/ml ethidium bromide in TAE buffer. DNA bands were visualized by UV exposure and photographed on a UV transilluminator. Fluorescent bands were quantitated by scanning the agarose gels on a Typhoon 9400 Variable Mode Imager (GE Healthcare).

Supercoiled DNA Relaxation Assay

TOP1 activity was measured, on the basis of the relaxation of supercoiled DNA, using the TOP1 assay kit (Topogen). DNA relaxation assay was performed according to the manufacturer's instruction. Reaction buffer, containing 10 mM Tris-HCl (pH 7.9), 150 mM NaCl, 1 mM EDTA, 0.1% BSA, 0.1 mM spermidine, and 5% glycerol, was mixed with 0.25 μg of supercoiled DNA, 4 units of human TOP1, and the indicated concentrations of the compounds in a total volume of 20 μl. After incubation at 37°C for 30 min, the reaction

was terminated with the addition of 2 μl 10% SDS. The reaction mixtures were treated with 50 μg/ml proteinase K for 30 min at 37°C to digest the protein. Two microliters of loading buffer was added, and the DNA was extracted once with CIA (chloroform:isoamyl alcohol, 24:1). Samples were resolved by electrophoresis on a 1% agarose gel, after which the gel was stained with 0.5 μg/ml ethidium bromide in TAE buffer for 30 min. DNA bands were visualized by UV exposure and photographed on a UV transilluminator.

Western Blot

Western blot was performed as described with slight modifications (Woo et al., 2006). Briefly, cell lysates were prepared in RIPA buffer (25 mM HEPES [pH 7.8], 0.5 M NaCl, 5 mM EDTA, 1.5% Triton X-100, 1.0% sodium deoxycholate, 0.1% SDS, and 5 mM EDTA), supplemented with a protease inhibitor cocktail (Roche). Samples were subjected to SDS-PAGE and transferred to a PVDF membrane (Immobilon P, Millipore). Membranes were incubated with the indicated primary antibodies and horseradish peroxidase–labeled secondary antibodies and visualized by exposure to X-ray film using SuperSignal West Pico Chemiluminescence Substrate (Pierce).

BNS-22 Binding Assay

BNS-22–immobilized beads were prepared as described elsewhere (Kanoh et al., 2005; Kawatani et al., 2008). Purified human TOP2α (500 ng) was incubated with control or BNS-22 beads (20 μl) in the presence or absence of 100 μM BNS-22 or 100 μM ICRF-193 in binding buffer containing 40 mM Tris-HCl (pH 7.5), 100 mM KCl, 10 mM $MgCl_2$, 0.5 mM EDTA, 5 mM DTT, 2 mM ATP, and 0.1% BSA in a total volume of 1 ml for 3 hr at 4°C. The reactant beads were washed with binding buffer without BSA, and the bound protein was eluted with SDS-PAGE sample buffer. The sample was resolved by SDS-PAGE and detected by western blot with anti-TOP2α.

SUPPLEMENTAL INFORMATION

Supplemental Information includes five figures, one table, and Supplemental Experimental Procedures and can be found with this article online at doi:10.1016/j.chembiol.2011.03.012.

ACKNOWLEDGMENTS

We thank Nippon Shinyaku Co., Ltd. for providing the compounds, H. Kondo and K. Noda for the proteome analysis, S. Kazami and K. Tomita for cell staining, H. Aono for cell culture, and K. Wierzba and T. Shimizu for critically reading the manuscript. This work was supported in part by a Grant-in-Aid from the Ministry of Education, Culture, Sports, Science, and Technology of Japan. The authors declare no competing financial interests.

Received: November 1, 2010
Revised: March 29, 2011
Accepted: March 30, 2011
Published: June 23, 2011

REFERENCES

Andoh, T., and Ishida, R. (1998). Catalytic inhibitors of DNA topoisomerase II. Biochim. Biophys. Acta *1400*, 155–171.

Austin, C.A., and Marsh, K.L. (1998). Eukaryotic DNA topoisomerase IIβ. Bioessays *20*, 215–226.

Bantscheff, M., Eberhard, D., Abraham, Y., Bastuck, S., Boesche, M., Hobson, S., Mathieson, T., Perrin, J., Raida, M., Rau, C., et al. (2007). Quantitative chemical proteomics reveals mechanisms of action of clinical ABL kinase inhibitors. Nat. Biotechnol. *25*, 1035–1044.

Bates, A.D., and Maxwell, A. (2007). Energy coupling in type II topoisomerases: why do they hydrolyze ATP? Biochemistry *46*, 7929–7941.

Berger, J.M., Gamblin, S.J., Harrison, S.C., and Wang, J.C. (1996). Structure and mechanism of DNA topoisomerase II. Nature *379*, 225–232.

Boyd, M.R., Farina, C., Belfiore, P., Gagliardi, S., Kim, J.W., Hayakawa, Y., Beutler, J.A., McKee, T.C., Bowman, B.J., and Bowman, E.J. (2001). Discovery of a novel antitumor benzolactone enamide class that selectively inhibits mammalian vacuolar-type (H^+)-ATPases. J. Pharmacol. Exp. Ther. *297*, 114–120.

Champoux, J.J. (2001). DNA topoisomerases: structure, function, and mechanism. Annu. Rev. Biochem. *70*, 369–413.

Chene, P., Rudloff, J., Schoepfer, J., Furet, P., Meier, P., Qian, Z., Schlaeppi, J.M., Schmitz, R., and Radimerski, T. (2009). Catalytic inhibition of topoisomerase II by a novel rationally designed ATP-competitive purine analogue. BMC Chem. Biol. *9*, 1.

Classen, S., Olland, S., and Berger, J.M. (2003). Structure of the topoisomerase II ATPase region and its mechanism of inhibition by the chemotherapeutic agent ICRF-187. Proc. Natl. Acad. Sci. USA *100*, 10629–10634.

Denny, W.A., and Baguley, B.C. (2003). Dual topoisomerase I/II inhibitors in cancer therapy. Curr. Top. Med. Chem. *3*, 339–353.

Figueiredo-Pereira, M.E., Chen, W.E., Li, J., and Johdo, O. (1996). The antitumor drug aclacinomycin A, which inhibits the degradation of ubiquitinated proteins, shows selectivity for the chymotrypsin-like activity of the bovine pituitary 20 S proteasome. J. Biol. Chem. *271*, 16455–16459.

Fortune, J.M., and Osheroff, N. (1998). Merbarone inhibits the catalytic activity of human topoisomerase IIα by blocking DNA cleavage. J. Biol. Chem. *273*, 17643–17650.

Gunther, E.C., Stone, D.J., Gerwien, R.W., Bento, P., and Heyes, M.P. (2003). Prediction of clinical drug efficacy by classification of drug-induced genomic expression profiles *in vitro*. Proc. Natl. Acad. Sci. USA *100*, 9608–9613.

Hajji, N., Pastor, N., Mateos, S., Dominguez, I., and Cortes, F. (2003). DNA strand breaks induced by the anti-topoisomerase II bis-dioxopiperazine ICRF-193. Mutat. Res. *530*, 35–46.

Huang, K.C., Gao, H., Yamasaki, E.F., Grabowski, D.R., Liu, S., Shen, L.L., Chan, K.K., Ganapathi, R., and Snapka, R.M. (2001). Topoisomerase II poisoning by ICRF-193. J. Biol. Chem. *276*, 44488–44494.

Isaacs, R.J., Davies, S.L., Sandri, M.I., Redwood, C., Wells, N.J., and Hickson, I.D. (1998). Physiological regulation of eukaryotic topoisomerase II. Biochim. Biophys. Acta *1400*, 121–137.

Ishida, R., Miki, T., Narita, T., Yui, R., Sato, M., Utsumi, K.R., Tanabe, K., and Andoh, T. (1991). Inhibition of intracellular topoisomerase II by antitumor bis(2,6-dioxopiperazine) derivatives: mode of cell growth inhibition distinct from that of cleavable complex-forming type inhibitors. Cancer Res. *51*, 4909–4916.

Jensen, P.B., Sorensen, B.S., Demant, E.J., Sehested, M., Jensen, P.S., Vindelov, L., and Hansen, H.H. (1990). Antagonistic effect of aclarubicin on the cytotoxicity of etoposide and 4′-(9-acridinylamino)methanesulfon-*m*-anisidide in human small cell lung cancer cell lines and on topoisomerase II-mediated DNA cleavage. Cancer Res. *50*, 3311–3316.

Jensen, L.H., Dejligbjerg, M., Hansen, L.T., Grauslund, M., Jensen, P.B., and Sehested, M. (2004). Characterisation of cytotoxicity and DNA damage induced by the topoisomerase II-directed bisdioxopiperazine anti-cancer agent ICRF-187 (dexrazoxane) in yeast and mammalian cells. BMC Pharmacol. *4*, 31.

Jensen, L.H., Thougaard, A.V., Grauslund, M., Sokilde, B., Carstensen, E.V., Dvinge, H.K., Scudiero, D.A., Jensen, P.B., Shoemaker, R.H., and Sehested, M. (2005). Substituted purine analogues define a novel structural class of catalytic topoisomerase II inhibitors. Cancer Res. *65*, 7470–7477.

Ju, B.G., Lunyak, V.V., Perissi, V., Garcia-Bassets, I., Rose, D.W., Glass, C.K., and Rosenfeld, M.G. (2006). A topoisomerase IIβ-mediated dsDNA break required for regulated transcription. Science *312*, 1798–1802.

Kanoh, N., Honda, K., Simizu, S., Muroi, M., and Osada, H. (2005). Photo-cross-linked small-molecule affinity matrix for facilitating forward and reverse chemical genetics. Angew. Chem. Int. Ed. Engl. *44*, 3559–3562.

Kawatani, M., Okumura, H., Honda, K., Kanoh, N., Muroi, M., Dohmae, N., Takami, M., Kitagawa, M., Futamura, Y., Imoto, M., et al. (2008). The identification of an osteoclastogenesis inhibitor through the inhibition of glyoxalase I. Proc. Natl. Acad. Sci. USA *105*, 11691–11696.

Kimura, S., Ito, C., Jyoko, N., Segawa, H., Kuroda, J., Okada, M., Adachi, S., Nakahata, T., Yuasa, T., Filho, V.C., et al. (2005). Inhibition of leukemic cell

growth by a novel anti-cancer drug (GUT-70) from *Calophyllum brasiliense* that acts by induction of apoptosis. Int. J. Cancer *113*, 158–165.

Lamb, J., Crawford, E.D., Peck, D., Modell, J.W., Blat, I.C., Wrobel, M.J., Lerner, J., Brunet, J.P., Subramanian, A., Ross, K.N., et al. (2006). The Connectivity Map: using gene-expression signatures to connect small molecules, genes, and disease. Science *313*, 1929–1935.

Larsen, A.K., and Skladanowski, A. (1998). Cellular resistance to topoisomerase-targeted drugs: from drug uptake to cell death. Biochim. Biophys. Acta *1400*, 257–274.

Larsen, A.K., Escargueil, A.E., and Skladanowski, A. (2003). Catalytic topoisomerase II inhibitors in cancer therapy. Pharmacol. Ther. *99*, 167–181.

Mao, Y., Desai, S.D., Ting, C.Y., Hwang, J., and Liu, L.F. (2001). 26 S proteasome-mediated degradation of topoisomerase II cleavable complexes. J. Biol. Chem. *276*, 40652–40658.

Muroi, M., Kazami, S., Noda, K., Kondo, H., Takayama, H., Kawatani, M., Usui, T., and Osada, H. (2010). Application of proteomic profiling based on 2D-DIGE for classification of compounds according to the mechanism of action. Chem. Biol. *17*, 460–470.

Nitiss, J.L. (2009a). DNA topoisomerase II and its growing repertoire of biological functions. Nat. Rev. Cancer *9*, 327–337.

Nitiss, J.L. (2009b). Targeting DNA topoisomerase II in cancer chemotherapy. Nat. Rev. Cancer *9*, 338–350.

Perlman, Z.E., Slack, M.D., Feng, Y., Mitchison, T.J., Wu, L.F., and Altschuler, S.J. (2004). Multidimensional drug profiling by automated microscopy. Science *306*, 1194–1198.

Pommier, Y., Leo, E., Zhang, H., and Marchand, C. (2010). DNA topoisomerases and their poisoning by anticancer and antibacterial drugs. Chem. Biol. *17*, 421–433.

Roca, J., Ishida, R., Berger, J.M., Andoh, T., and Wang, J.C. (1994). Antitumor bisdioxopiperazines inhibit yeast DNA topoisomerase II by trapping the enzyme in the form of a closed protein clamp. Proc. Natl. Acad. Sci. USA *91*, 1781–1785.

Rogakou, E.P., Pilch, D.R., Orr, A.H., Ivanova, V.S., and Bonner, W.M. (1998). DNA double-stranded breaks induce histone H2AX phosphorylation on serine 139. J. Biol. Chem. *273*, 5858–5868.

Sorensen, B.S., Sinding, J., Andersen, A.H., Alsner, J., Jensen, P.B., and Westergaard, O. (1992). Mode of action of topoisomerase II-targeting agents at a specific DNA sequence. Uncoupling the DNA binding, cleavage and religation events. J. Mol. Biol. *228*, 778–786.

Tanabe, K., Ikegami, Y., Ishida, R., and Andoh, T. (1991). Inhibition of topoisomerase II by antitumor agents bis(2,6-dioxopiperazine) derivatives. Cancer Res. *51*, 4903–4908.

Teruya, T., Simizu, S., Kanoh, N., and Osada, H. (2005). Phoslactomycin targets cysteine-269 of the protein phosphatase 2A catalytic subunit in cells. FEBS Lett. *579*, 2463–2468.

Umemura, K., Yanase, K., Suzuki, M., Okutani, K., Yamori, T., and Andoh, T. (2003). Inhibition of DNA topoisomerases I and II, and growth inhibition of human cancer cell lines by a marine microalgal polysaccharide. Biochem. Pharmacol. *66*, 481–487.

Usui, T., Watanabe, H., Nakayama, H., Tada, Y., Kanoh, N., Kondoh, M., Asao, T., Takio, K., Watanabe, H., Nishikawa, K., et al. (2004). The anticancer natural product pironetin selectively targets Lys352 of α-tubulin. Chem. Biol. *11*, 799–806.

Wang, J.C. (2002). Cellular roles of DNA topoisomerases: a molecular perspective. Nat. Rev. Mol. Cell Biol. *3*, 430–440.

Wilstermann, A.M., and Osheroff, N. (2003). Stabilization of eukaryotic topoisomerase II-DNA cleavage complexes. Curr. Top. Med. Chem. *3*, 321–338.

Woo, J.-T., Kawatani, M., Kato, M., Shinki, T., Yonezawa, T., Kanoh, N., Nakagawa, H., Takami, M., Lee, K.H., Stern, P.H., et al. (2006). Reveromycin A, an agent for osteoporosis, inhibits bone resorption by inducing apoptosis specifically in osteoclasts. Proc. Natl. Acad. Sci. USA *103*, 4729–4734.

Xiao, H., Mao, Y., Desai, S.D., Zhou, N., Ting, C.Y., Hwang, J., and Liu, L.F. (2003). The topoisomerase IIβ circular clamp arrests transcription and signals a 26S proteasome pathway. Proc. Natl. Acad. Sci. USA *100*, 3239–3244.

Yaguchi, S., Fukui, Y., Koshimizu, I., Yoshimi, H., Matsuno, T., Gouda, H., Hirono, S., Yamazaki, K., and Yamori, T. (2006). Antitumor activity of ZSTK474, a new phosphatidylinositol 3-kinase inhibitor. J. Natl. Cancer Inst. *98*, 545–556.

Yang, X., Li, W., Prescott, E.D., Burden, S.J., and Wang, J.C. (2000). DNA topoisomerase IIβ and neural development. Science *287*, 131–134.

Young, D.W., Bender, A., Hoyt, J., McWhinnie, E., Chirn, G.W., Tao, C.Y., Tallarico, J.A., Labow, M., Jenkins, J.L., Mitchison, T.J., et al. (2008). Integrating high-content screening and ligand-target prediction to identify mechanism of action. Nat. Chem. Biol. *4*, 59–68.